

RKCL4047

## KINETICS OF RHENIUM DIOXIDE DEPOSITION ON COLUMNAR STRUCTURED PLATINUM ELECTRODES

**Eduardo Méndez<sup>a</sup>, María F. Cerdá<sup>a</sup>, Carlos F. Zinola<sup>a</sup>,  
Ana M. Castro Luna<sup>b</sup> and María E. Martins<sup>b\*</sup>**

<sup>a</sup> Laboratorio de Electroquímica Fundamental y Bioelectroquímica. Facultad de Ciencias.  
Universidad de la República. Iguá 4225. 11400 Montevideo, Uruguay.

<sup>b</sup> Instituto de Investigaciones Fisicoquímicas Teóricas y Aplicadas (INIFTA). Universidad  
Nacional de La Plata. Suc. 4, CC16 (1900) La Plata, Argentina.

*Received December 12, 2001*

*In revised form May 21, 2002*

*Accepted July 15, 2002*

---

### Abstract

The kinetics concerning the early stage of the electrodeposition of rhenium dioxide on columnar-structured platinum electrodes from acid aqueous containing perrhenate ions was studied. The results demonstrate a zero-order kinetics obtained by holding the potential at two different values.

*Keywords:* Deposition, platinum electrodes, rhenium dioxide

---

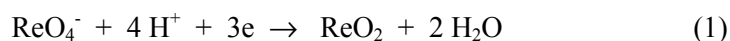
## INTRODUCTION

The electrodeposition of rhenium species on noble substrates has gained attention during the last years due to its possible application in binary electrodes [1-4]. The electrodeposition process on platinum can be achieved either by potentiostatic [5] or galvanostatic [6-9] procedures. In both cases, the early stages of the electrodeposition process result in the formation of a monolayer of rhenium species [5], but for longer times the development of multilayers takes place [9]. The multilayer rhenium-covered electrode consists of a mixture of rhenium oxides, as demonstrated by comparison of the voltammetric behavior of pure rhenium oxides and of the rhenium-covered electrode [9].

---

\* Corresponding author. E-mail: mmartins@inifta.unlp.edu.ar

The initial step of the electrodeposition of rhenium species on platinum electrodes leads to the formation of  $\text{ReO}_2$  as the main reaction product [5-10]. Nevertheless, whether this reaction can be achieved by direct electron transfer (eq. 1) or through the participation of pre-adsorbed hydrogen atoms ( $\text{H}_{\text{ad}}$ ) (eq. 2) is still a matter of discussion:



The use of different metals shed some light on this issue. For gold electrodes, on which only minute amounts of hydrogen atoms can be adsorbed, electrochemical quartz microbalance studies showed that perrhenate electroreduction occurs at more negative potential values than that at which the hydrogen evolution reaction (HER) takes place [11-13], suggesting that  $\text{H}_2$  was the reducing agent. On this electrode, metallic rhenium was identified as the electrodeposited species by SEM-EDS [12] and ellipsometry [13]. This case is suitable for a direct electron transfer mechanism (eq.1), which is reinforced by the fact that the industrial production of metallic rhenium is achieved by bubbling a stream of  $\text{H}_2$  into an aqueous solution of perrhenate.

Furthermore, for Pt electrodes, a metal capable to adsorb hydrogen atoms, the second mechanism in which  $\text{H}_{\text{ad}}$  are postulated to reduce perrhenate ions (eq. 2) may be considered appropriated. Szabó and Bakos [8] found that  $\text{ReO}_2$  electrodeposition on Pt could be achieved by the ionization of preadsorbed hydrogen atoms formed either in acid media or from methanol electrooxidation.

In order to acquire a deeper knowledge concerning the participation of  $\text{H}_{\text{ad}}$  in the early stages of rhenium species electrodeposition on Pt, two approaches have been essayed. First, the use of columnar-structured platinum electrodes (*cs*-Pt) which, because of their surface topography [14-17], allow an adequate handling of the variables related with mass transfer of perrhenate ions from the solution towards the electrode surface, and also of the surface sites available for both the rhenium species deposition and the electrosorption of hydrogen atoms. Second, a kinetic model involving the participation of  $\text{H}_{\text{ad}}$  has been tested to support the experimental findings. The experiments have been performed at two potential values located within the H-electrosorption potential domain.

## EXPERIMENTAL

The columnar structured platinum working electrode, *cs*-Pt (real area  $5 \text{ cm}^2$ ) was prepared from a polycrystalline Pt wire (Goodfellow, 99.999 %). The preparation technique consists of two stages [18-20]. The first one implies the

accumulation of a hydrous platinum oxide layer on the starting Pt electrode, through the application of a repetitive square wave potential routine at 4 kHz between 0.05 V and 2.40 V for a time  $t$ . The second stage involves the electroreduction of the hydrous oxide with a potentiodynamic sweep from 1.45 V down to 0 V at  $0.001 \text{ V s}^{-1}$  to produce the *cs*-Pt.

The supporting electrolyte was aqueous 1 M sulfuric acid prepared from T.J. Baker, ACS reagent with Millipore Milli-Q\* Plus water. Aqueous rhenium-containing solutions,  $10^{-3} \text{ M}$  (working solution), were prepared by dissolving  $\text{NH}_4\text{ReO}_4$  (Aldrich, 99 + %) in the supporting electrolyte.

A large area Pt wire and a reversible hydrogen electrode (RHE) were the counterelectrode and reference electrode, respectively. Potentials in the text are given on the RHE scale. All runs were performed at room temperature under nitrogen (99.998 %) atmosphere.

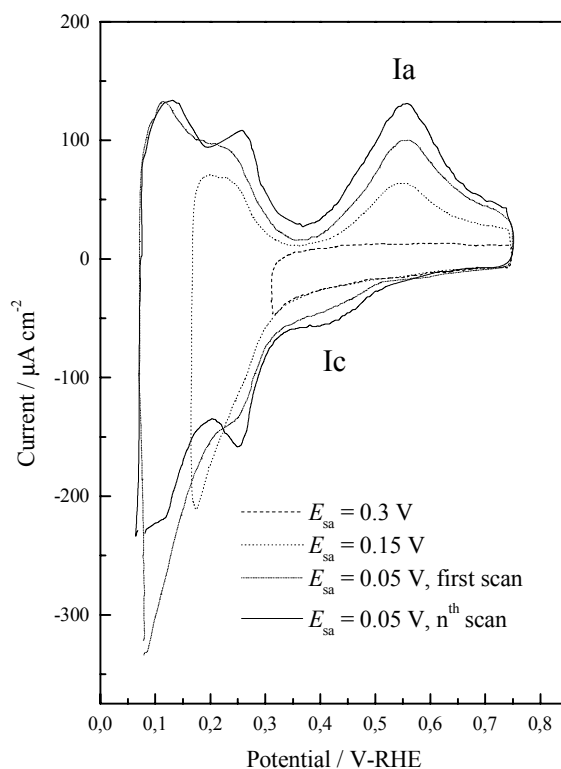


**Fig. 1.** Open window voltammograms for *cs*-Pt in  $10^{-3} \text{ M}$  aqueous perrenate +  $1 \text{ M H}_2\text{SO}_4$ .  $\nu = 0.10 \text{ V s}^{-1}$ ,  $A = 5 \text{ cm}^2$

Triangular potential sweeps (TPS) from  $E_{sc} = 0.05$  V to  $E_{sa} = 1.5$  V, and TPS including a potential holding at  $E_h = 0.25$  V and  $E_h = 0.15$  V were performed, both applied for times ( $t_h$ ) between 10 s and 180 s. The controlled hydrodynamic experiments were performed on *cs*-Pt ring-disc electrodes, prepared as mentioned above.

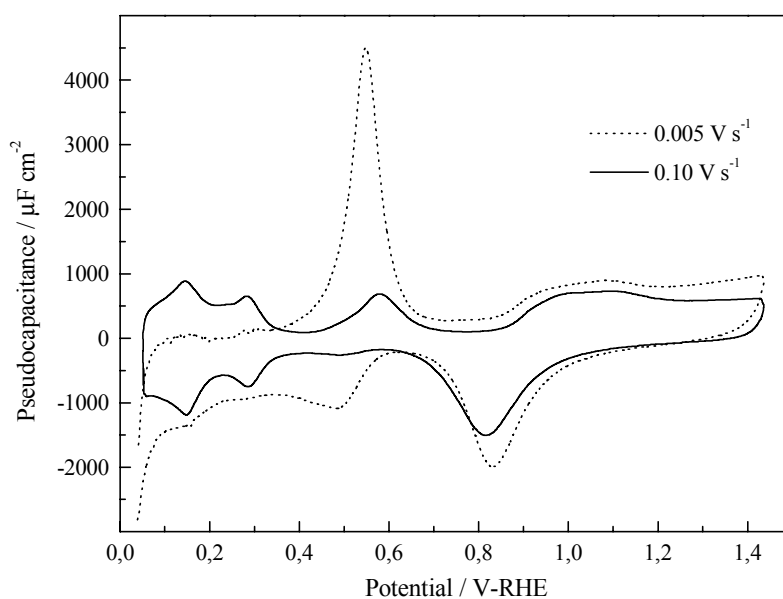


**Fig. 2.** Repetitive pseudocapacitance curves for the *cs*-Pt in  $10^{-3}$  M  $\text{NH}_4\text{ReO}_4$  + 1 M  $\text{H}_2\text{SO}_4$ .  $\nu = 0.005$  and  $0.10$   $\text{V s}^{-1}$ .  $A = 5$   $\text{cm}^2$

## RESULTS AND DISCUSSION

A clean *cs*-Pt electrode immersed in the working solution at 0.70 V and subjected subsequently to a potential cycling with a progressive decrease of the lower limit of the potential window ( $E_{sc}$ ), show that no anodic current peak develops prior to  $E_{sc} = 0.25$  V (Fig. 1). This result suggests that under potentiodynamic conditions the requirement to supply  $\text{H}_{ad}$  to form  $\text{ReO}_2$  is fulfilled. However, if the same experiment is repeated but a potential cycling in the 0.05 to 1.5 V range is previously performed, an anodic current peak is

obtained independently of the value of  $E_{sc}$  (Fig. 1, full line). The anodic charge density related to the stripping of  $\text{ReO}_2$  performed at  $0.1 \text{ V s}^{-1}$  resulted equal to  $(100 \pm 10) \mu\text{C cm}^{-2}$ .

Moreover, regarding the surface topography of the *cs*-Pt electrode that may allow the occurrence of  $\text{H}_{ad}$  and/or  $\text{ReO}_2$  deposition, depending on the potential sweep rate ( $\nu$ ) at which the experiment is performed, it was thought about the necessity to find a suitable  $\nu$  permitting the development of the two reactions on the same electrode. Thus, the results indicate that either a coverage of a submonolayer of  $\text{ReO}_2$  or a complete coverage by rhenium species at  $\nu = 0.1 \text{ V s}^{-1}$  and  $0.005 \text{ V s}^{-1}$ , respectively, is achieved (Fig. 2). These findings can be explained taking into account the diffusion of perrhenate ions to the columnar topography of the electrode. At high  $\nu$ , perrhenate ions only reach the tips of the columns, leaving the voids free for hydrogen adsorption, while at lower  $\nu$  the voids are also filled with perrhenate ions and the reduction reaction can take place. Consequently, the amount of  $\text{ReO}_2$  obtained under potentiodynamic conditions increases as  $\nu$  decreases.

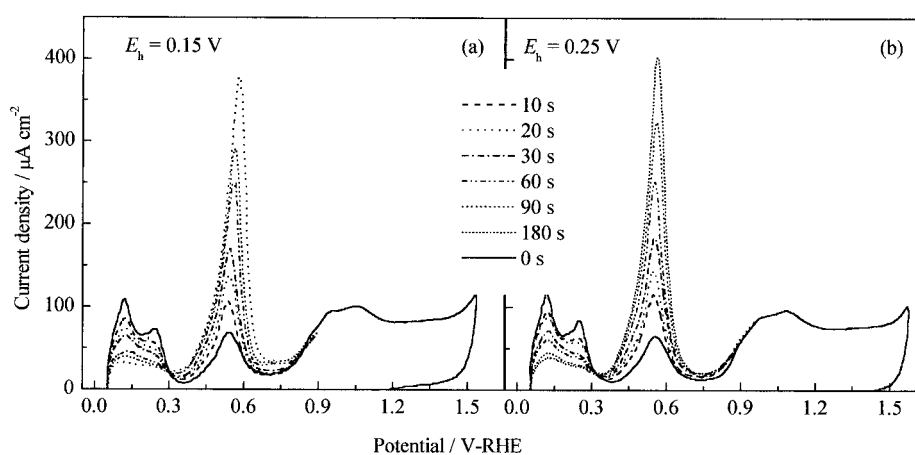


**Fig. 3.** Repetitive voltammogram for *cs*-Pt in  $10^{-3}$  M aqueous perrhenate + 1 M  $\text{H}_2\text{SO}_4$  (full line) and stripping curves after holding the potential at (a)  $E_h = 0.15 \text{ V}$  and (b)  $E_h = 0.25 \text{ V}$ , for  $10 \text{ s} \leq t_h \leq 180 \text{ s}$ .  $A = 5 \text{ cm}^2$ .

Once the experimental conditions to perform the potentiostatic deposition of rhenium species have been acquired, the study was carried out at two selected potentials ( $E_h$ ). The cyclic voltammograms corresponding to the stripping of the  $\text{ReO}_2$  formed on the *cs*-Pt electrode at  $E_h = 0.15$  V and 0.25 V are shown in Figs 3a and b, respectively. The stabilized voltammograms in the working solution ( $t_h = 0$ ) for both  $E_h$  (full line) show cathodic and anodic current peaks located at 0.46 V and 0.55 V, respectively. These current peaks result from the early stages in the electroformation and electrodisolution of adsorbed  $\text{ReO}_2$  at a submonolayer level during the initial potential cycling [5]. The anodic charge density at  $t_h = 0$  is equal to  $(100 \pm 10) \mu\text{C cm}^{-2}$  for both  $E_h$  values. For a constant  $E_h$ , the anodic charge density related to the electrooxidation of  $\text{ReO}_2$  to  $\text{ReO}_4^-$  increases with  $t_h$ , indicating that a larger quantity of  $\text{ReO}_2$  has been formed. Accordingly, the charge density related to the H-electrosorption reaction decreases as  $t_h$  increases due to the blocking coverage of the *cs*-Pt surface by  $\text{ReO}_2$  species. At  $E_h = 0.15$  V, the anodic peak potential shifts towards positive values for  $t_h > 60$  s, whereas for  $E_h = 0.25$  V, no shift of the potential peak is observed in the whole  $t_h$  range. For  $E > 0.7$  V, the  $\text{ReO}_2$  species are completely stripped from the surface, as deduced from the undistorted O-electrosorption profile.

According to eq. 2, the kinetic equation related to the formation of  $\text{ReO}_2$  can be written as:

$$\frac{dQ_{\text{ReO}_2}}{dt} = k[\text{ReO}_4^-][\text{H}^+]\theta_H^3 \quad (3)$$

where  $k$  is the kinetic constant,  $Q_{\text{ReO}_2}$  is the anodic charge density involved in the electrooxidation of  $\text{ReO}_2$  to  $\text{ReO}_4^-$ , and  $\theta_H$  is the degree of coverage of *cs*-Pt surface with  $\text{H}_{\text{ad}}$ . The value of  $\theta_H$  depends on  $E_h$ , and it is constant for each  $E_h$  value because the H electrosorption reaction is very fast [21]. In addition, although  $\text{H}_{\text{ad}}$  are consumed while the reaction takes place, at  $E \geq 0.15$  V the electrode surface has not yet achieved a complete coverage by these species, allowing the continuous renewal of  $\text{H}_{\text{ad}}$  as soon as they are consumed. Thus, at a fixed  $E_h$  all the factors at the right hand of eq. 3 are considered as constant ones.

Integration of eq. 3 leads to:

$$Q_{\text{ReO}_2} = Q_{\text{ReO}_2}^o + k' \cdot t_h \quad (4)$$

where  $Q_{\text{ReO}_2}^o$  stands for the anodic charge density at  $t_h = 0$ , and  $k' \equiv k[\text{ReO}_4^-][\text{H}^+]\theta_H^3$ . This zero-order kinetic model explains why the reaction does not occur in a large extent in basic media [10], as both  $[\text{H}^+]$  and  $\theta_H$  decrease significantly with the increase of pH.

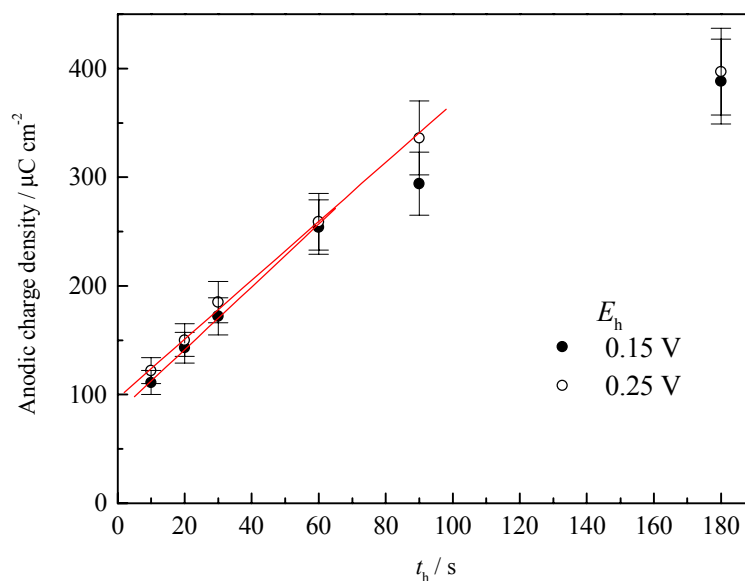


**Fig. 4.** Anodic charge density vs  $t_h$  plot for  $E_h = 0.15 \text{ V}$  and  $0.25 \text{ V}$

The evolution of  $Q_{\text{ReO}_2}$  with  $t_h$  is shown in Fig. 4. For  $E_h = 0.15 \text{ V}$ , a linear relationship is obtained for  $t_h \leq 60 \text{ s}$ , while for  $E_h = 0.25 \text{ V}$ , the linear relationship is verified only for  $t_h \leq 90 \text{ s}$ . The slopes of the linear ranges ( $k'$ ) are  $(2.9 \pm 0.1) \mu\text{C cm}^{-2} \text{ s}^{-1}$  and  $(2.7 \pm 0.1) \mu\text{C cm}^{-2} \text{ s}^{-1}$ , for  $E_h = 0.15 \text{ V}$  and  $0.25 \text{ V}$ , respectively. The intercepts of  $Q_{\text{ReO}_2}$  at  $t_h = 0$ ,  $Q_{\text{ReO}_2}^0$  are  $(83 \pm 2) \mu\text{C cm}^{-2}$  and  $(97 \pm 3) \mu\text{C cm}^{-2}$ , the latter being in close agreement with that found experimentally.

It should be emphasized that the  $t_h$  range in which eq. 3 is valid is larger for  $E_h = 0.25 \text{ V}$  as compared with  $E_h = 0.15 \text{ V}$ . This fact can be explained by taking into account that the only reaction occurring at  $E_h = 0.25 \text{ V}$  is the one described by eq. 2, whereas at  $E_h = 0.15 \text{ V}$ , two processes may be competing. In order to ascertain with this hypothesis, a rotating ring-disc electrode has been used to detect any soluble rhenium species that could have been formed. An anodic current is obtained when the ring potential is set at  $0.60 \text{ V}$  (Fig. 5), denoting the formation of a soluble species at  $0.15 \text{ V}$ , probably a  $\text{Re(III)}$ -soluble species

[22]. This fact explains for what reason the zero order kinetic model is accomplished by the data obtained at  $E_h = 0.15$  V, although a slight departure between the predicted and the experimental values of  $Q_{\text{ReO}_2}^0$  is observed.

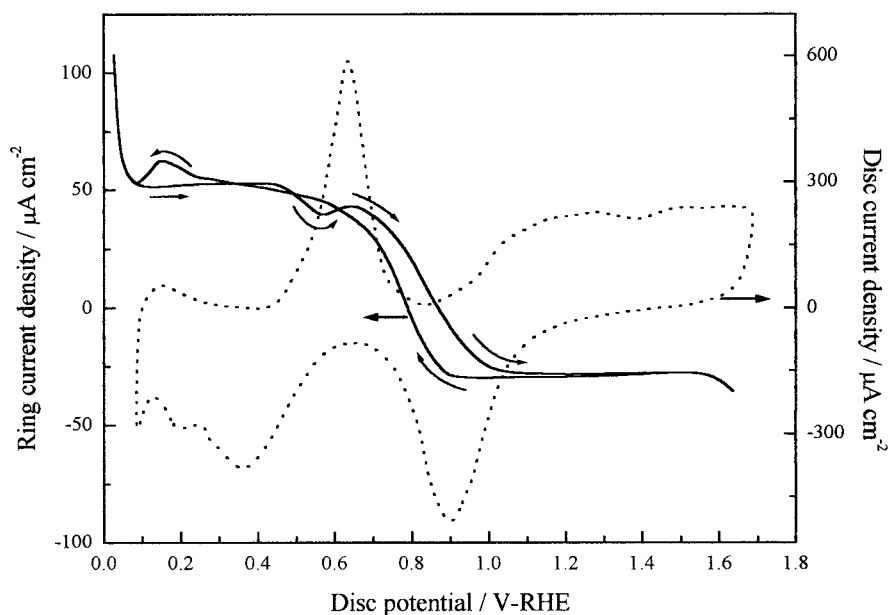


**Fig. 5.** Ring and disc current densities during the application of a triangular potential sweep to the ring at  $0.10 \text{ V s}^{-1}$  in the working solution.  $E_{\text{ring}} = 0.60 \text{ V}$ ,  $A_{\text{disc}} = 3.24 \text{ cm}^2$ ,  $A_{\text{ring}} = 0.76 \text{ cm}^2$

Moreover, the deviations detected from the proposed kinetic model deserve a particular consideration. These deviations are observed for  $t_h > 90$  s at  $E_h = 0.25$  V, and for  $t_h > 60$  s at  $E_h = 0.15$  V. At  $E_h = 0.25$  V, this depart could be attributed to the formation of multilayers of adsorbed  $\text{ReO}_2$  [9]. However, at  $E_h = 0.15$  V, the formation of  $\text{Re(III)}$ -soluble species and its further oxidation to  $\text{ReO}_2$  should account for the non-applicability of the kinetic model at an extended  $t_h$  range. The oxidation of  $\text{Re(III)}$ -soluble species during the positive going potential scan produces  $\text{ReO}_2$  on the previously deposited  $\text{ReO}_2$ , probably in a multilayer fashion. In this sense, the anodic charge density increases,



preserving an almost constant value for the H-electrosorption charge density, explaining the deviations observed in Fig. 4. The formation of multilayers of adsorbed  $\text{ReO}_2$  also agrees with the shift of the anodic peak potential observed in Fig. 3.

From the results presented in this work, the following conclusions can be drawn:

1. A kinetic model for the deposition of  $\text{ReO}_2$  from acid aqueous containing perrhenate ions on *cs*-Pt electrodes was developed, which takes into account the participation of  $\text{H}_{\text{ad}}$  in the reduction process.
2. The kinetic model fits the experimental values obtained at  $E_{\text{h}} = 0.25$  V, potential at which the reduction of perrhenate ion takes place (eq. 2).
3. Data obtained at  $E_{\text{h}} = 0.15$  V fit the kinetic model, but the predicted values deviate slightly from the experimental ones. At this potential, a partial reduction of  $\text{ReO}_2$  to  $\text{Re(III)}$ -soluble species occurs, which oxidizes to  $\text{ReO}_2$  in the positive going potential sweep, accumulating in a multilayer fashion.
4. For prolonged  $t_{\text{h}}$ , a  $\text{ReO}_2$  multilayer formation takes place, in accordance to other reports [9].

**Acknowledgements.** Financial support for this work was obtained from PEDECIBA (PNUD/URU), Fondo Clemente Estable FCE 6015 (Uruguay), and Agencia Nacional de Promoción Científica y Tecnológica (Argentina).

## REFERENCES

1. C.G. Michel, W.E. Bambrick, R.H. Ebel, G. Larsen, G.L. Haller: *J. Catal.*, **154**, 222 (1995).
2. B.N. Grgur, N.M. Markovic, P.N. Ross: *Electrochim. Acta*, **43**, 3631 (1998).
3. W. Juszczyk, Z. Karpinski: *Appl. Catal. A.*, **206**, 67 (2001).
4. R. Schrebler, M. Merino, P. Cury, M. Romo, R. Córdova, H. Gómez, E.A. Dalchiele: *Thin Solid Films*, **388**, 201 (2001).
5. R. Schrebler, H. Gómez, R. Córdova: *Electrochim. Acta*, **34**, 1405 (1989).
6. I. Bakos, G. Horányi: *J. Electroanal. Chem.*, **375**, 387 (1994).
7. S. Szabó, I. Bakos: *React. Kinet. Catal. Lett.*, **62**, 267 (1997).
8. S. Szabó, I. Bakos: *React. Kinet. Catal. Lett.*, **65**, 259 (1998).
9. S. Szabó, I. Bakos: *J. Electroanal. Chem.*, **492**, 103 (2000).
10. G.A. Mazzocchin, F. Magno, G. Bontempelli: *Inorg. Chim. Acta*, **13**, 209 (1975).
11. G. Horányi, I. Bakos: *J. Electroanal. Chem.*, **378**, 143 (1994).
12. R. Schrebler, P. Cury, M. Orellana, H. Gómez, R. Córdova, E.A. Dalchiele: *Electrochim. Acta*, **46**, 4309 (2001).
13. J. Zerbino, A.M. Castro Luna, C.F. Zinola, E. Méndez, M.E. Martins: *J. Electroanal. Chem.*, **521**, 763 (2002).
14. L. Vázquez, J. Gómez, A.M. Baró, N. García, M.L. Marcos, J. González Velasco, J.M. Vara, A.J. Arvia, J. Presa, A. García, M. Aguilar: *J. Am. Chem. Soc.*, **109**, 1731 (1987).

15. C. Alonso, R.C. Salvarezza, J.M. Vara, A.J. Arvia, L. Vázquez, A. Bartolomé, A.M. Baró: *J. Electrochem. Soc.*, **137**, 2161 (1990).
16. M.E. Martins, F.J. Rodríguez Nieto, R.C. Salvarezza, G. Andreassen, A.J. Arvia: *J. Electroanal. Chem.*, **477**, 14 (1999).
17. J. Zerbino, C.L. Perdriel, A.J. Arvia: *Thin Solid Films*, **232**, 63 (1993).
18. A. Chialvo, W.E. Triaca, A.J. Arvia: *J. Electroanal. Chem.*, **146**, 93 (1983).
19. A.J. Arvia, R.C. Salvarezza, W.E. Triaca: *Electrochim. Acta*, **34**, 1057 (1989).
20. A. Visintin, R.C. Salvarezza, W.E. Triaca: *J. Electroanal. Chem.*, **284**, 465 (1990).
21. A. Frumkin: *Advances in Electrochemistry and Electrochemical Engineering*. Eds. P. Delahay, C. Tobias, Chapter 3. New York 1963.
22. J. Gómez, J.I. Gardiazábal, R. Schrebler, H. Gómez, R. Ccordova: *J. Electroanal. Chem.*, **260**, 113 (1989).